Supplementary Materials

Robust generation of erythroid and multilineage hematopoietic progenitors from human iPSCs using a scalable monolayer culture system

Juan Pablo Ruiz[a], Guibin Chen[b], Juan Jesus Haro Mora[a], Keyvan Keyvanfar[c], Chengyu Liu[d], Jizhong Zou[e], Jeanette Beers[e], Hanan Bloomer[a], Husam Qanash[a,f,g] Naoya Uchida[a], John F. Tisdale[a], Manfred Boehm[b], Andre Larochelle[a*]

Affiliations:

[a]Cellular and Molecular Therapeutics Branch, National Heart, Lung and Blood Institute (NHLBI), National Institutes of Health (NIH), Bethesda, MD 20892, USA.

[b]Translational Vascular Medicine Branch, NHLBI, NIH, Bethesda, MD 20892, USA.

[c]Clinical Flow Core Facility, NHLBI, NIH, Bethesda, MD 20892, USA.

[d]Transgenic Core Facility, NHLBI, NIH, Bethesda, MD 20892, USA.

[e]iPSC Core Facility, NHLBI, NIH, Bethesda, MD 20892, USA.

[f]College of Applied Medical Sciences, University of Hail, Hail, Saudi Arabia.

[g]Department of Biology, The Catholic University of America, Washington, DC 20064, USA.

Author list footnotes:

*** Corresponding author:** Andre Larochelle, M.D. Ph.D., National Heart, Lung and Blood Institute, National Institutes of Health, Bethesda, 9000 Rockville, Bethesda, MD 20892, USA.

☎ (301) 451-7139 larochea@nhlbi.nih.gov (301) 496-8396

This PDF file includes:

Figures S1-S6
Tables S1-S3

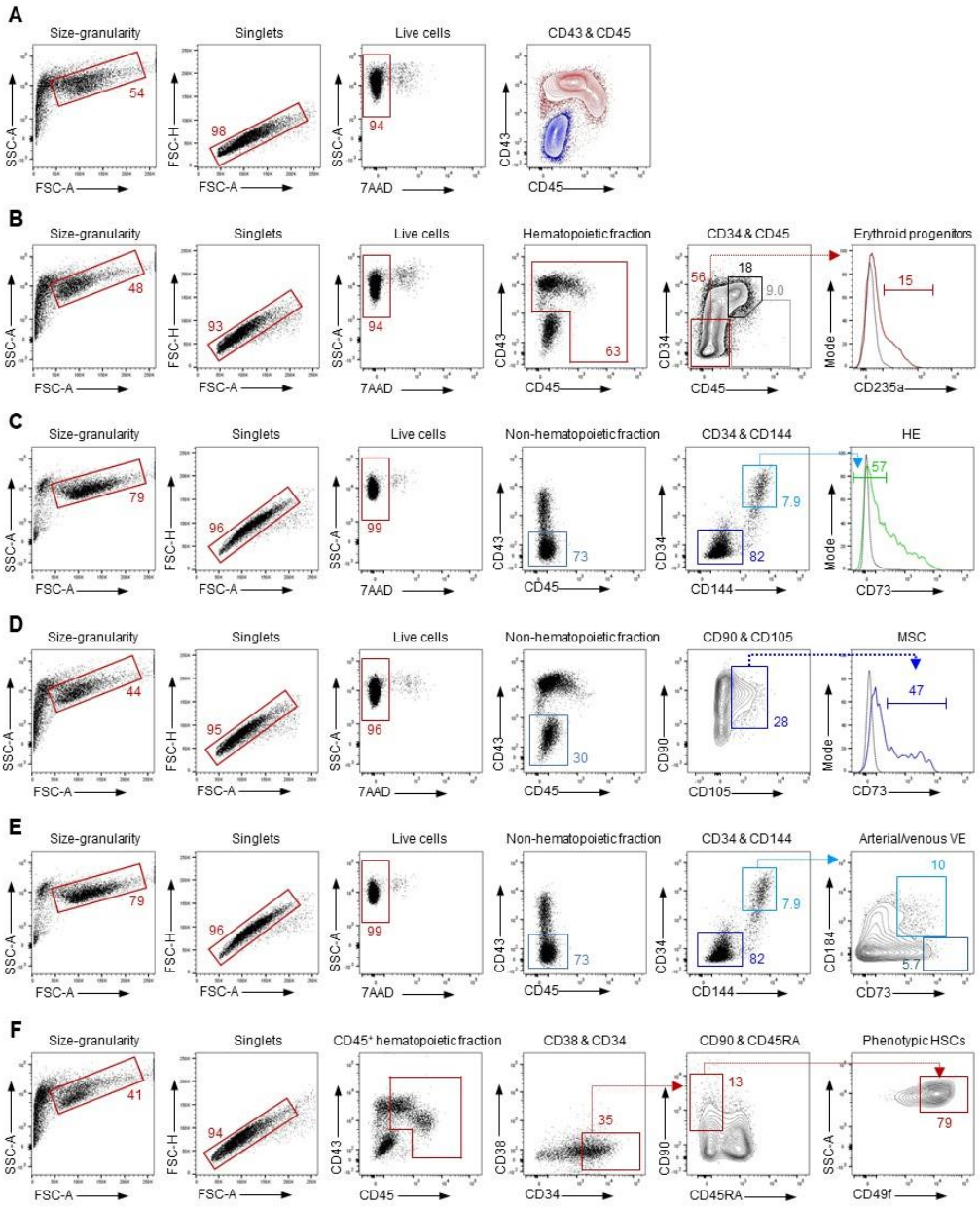

Figure S1 | Complete gating strategies used for flow cytometry characterization of the cellular constituents arising during human iPSC differentiation with STEMdiff™ hematopoietic kit. (**A**) Representative gating strategy for hematopoietic and non-hematopoietic fractions at day 12 of differentiation; associated with Fig. 1C. (**B**) Representative gating strategy for hematopoietic populations at day 10 of differentiation; associated with Fig. 2A. (**C**) Representative gating strategy for populations of mesenchymal cells, vascular endothelium (VE) and hemogenic endothelium (HE) at day 5 of differentiation; associated with Fig. 3A. (**D**) Representative gating strategy for populations of mesenchymal stromal cells (MSC) at day 10 of differentiation; associated with Fig. 3C. (**E**) Representative gating strategy for populations of arterial and venous VE at day 5 of differentiation; associated with Fig. 3F. (**F**) Representative gating strategy for populations of immunophenotypic HSCs at day 12 of differentiation; associated with Fig. S4A.

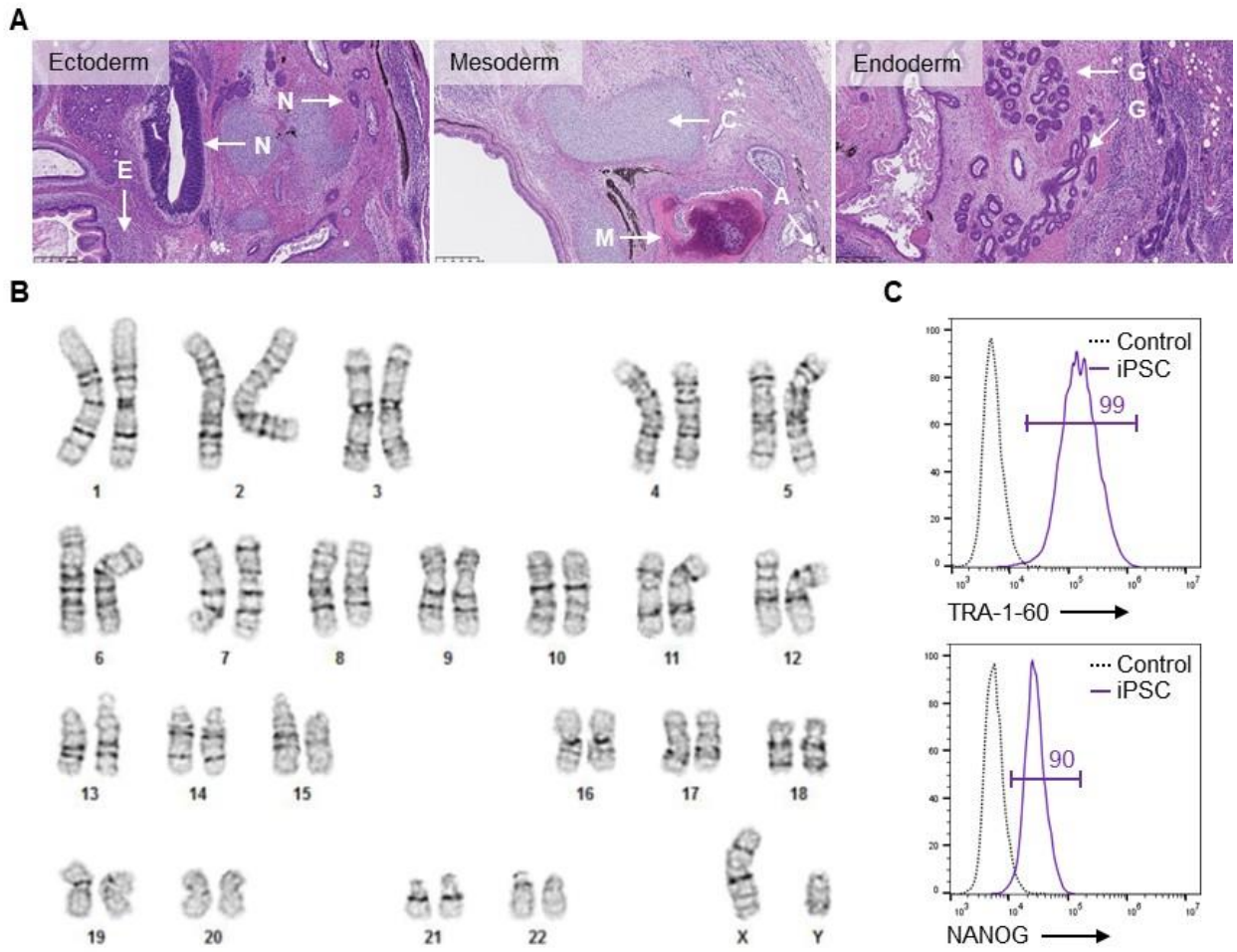

Figure S2 | Characterization of MCND-TENS2 iPSC line. (**A**) Hematoxylin and eosin stain of a teratoma from MCND-TENS2 iPSCs, displaying structures representative of ectoderm, mesoderm and endoderm. E, epidermal tissue; N, neutral tissue; M, striated muscle; C, cartilage; A, adipose tissue; G, gut epithelial tissue. Scale bar = 250 µm. (**B**) Cytogenetic analysis showing a normal karyotype (46, XY). (**C**) Flow cytometry analysis of iPSCs showing expression of pluripotency protein markers, TRA-1-60 and NANOG, compared to isotype controls.

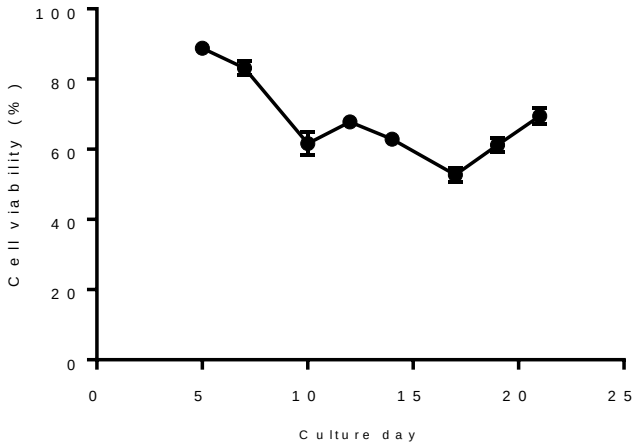

Figure S3 | Cell viability during human iPSC differentiation with STEMdiff™ hematopoietic kit. Total cell viability was measured by acridine orange (AO)/propidium iodide (PI) staining for each sample throughout differentiation. Results are shown as mean ± SEM (n=8). Associated with Fig. 1E.

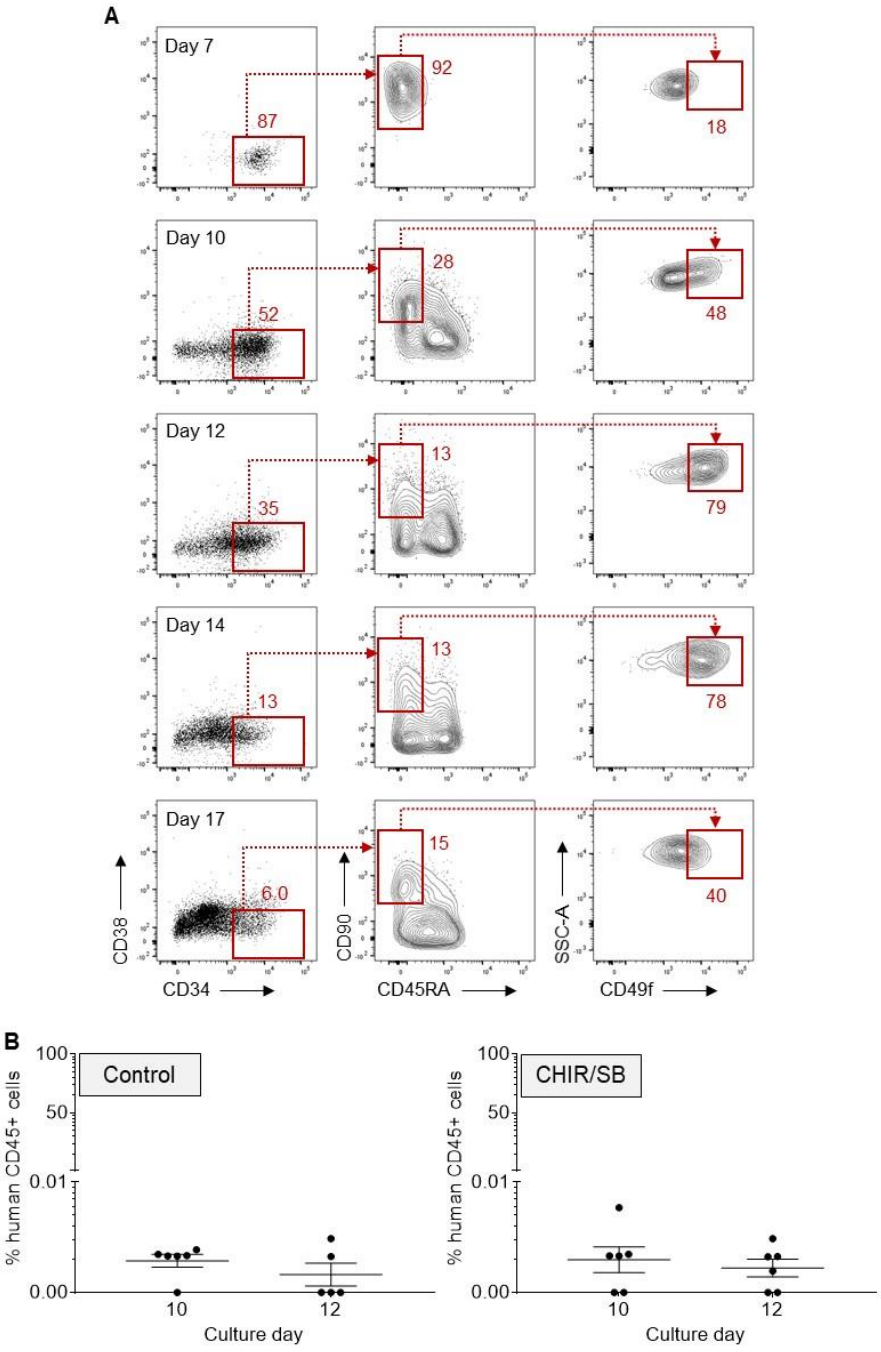

Figure S4 | Production of immunophenotypic HSCs with no long-term engraftment potential during human iPSC differentiation with STEMdiff™ hematopoietic kit. (**A**) Representative flow cytometry plots depicting $CD34^{+}CD38^{-}CD45RA^{-}CD90^{+}CD49f^{+}$ cells in gated $CD43^{+}CD45^{+}$ hematopoietic cells at various days of differentiation. The complete gating strategy is shown in Fig. S1F. (**B**) Human cell engraftment depicted as percentage of human CD45-expressing cells in the bone marrow of recipient NSG mice 16 weeks after transplantation of day 10 or 12 sorted $CD43^{+}CD45^{+}$ hematopoietic cells derived from control (left panel, associated with Fig. 2E) or CHIR/SB-supplemented cultures (right panel, associated with Fig. 5G). Results are shown as mean ± SEM; each dot represents an individual mouse (n= 5 to 6 mice per group).

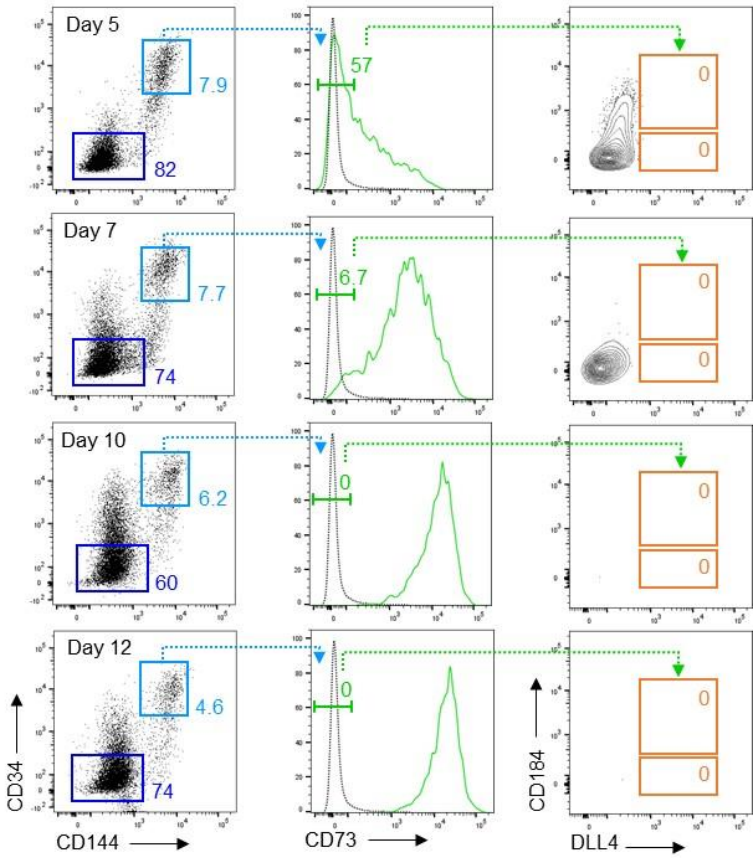

Figure S5 | Limited hemogenic endothelium (HE) and arterial-type HE formation during human iPSC differentiation with STEMdiff™ hematopoietic kit. Representative flow cytometry plots of CD34, CD144 (VE-cadherin), CD73, DLL4 and CD184 expression in gated $CD43^{-}CD45^{-}$ non-hematopoietic cells at various days of differentiation. Gates shown include: $CD144^{-}CD34^{-}$ mesenchymal cells (dark blue), $CD144^{+}CD34^{hi}$ vascular endothelium (VE, light blue), $CD144^{+}CD34^{hi}CD73^{-}$ hemogenic endothelium (HE, green), and $CD144^{+}CD34^{hi}CD73^{-}DLL4^{+}CD184^{+/-}$ arterial-type HE. The complete gating strategy is shown in Fig. S1C.

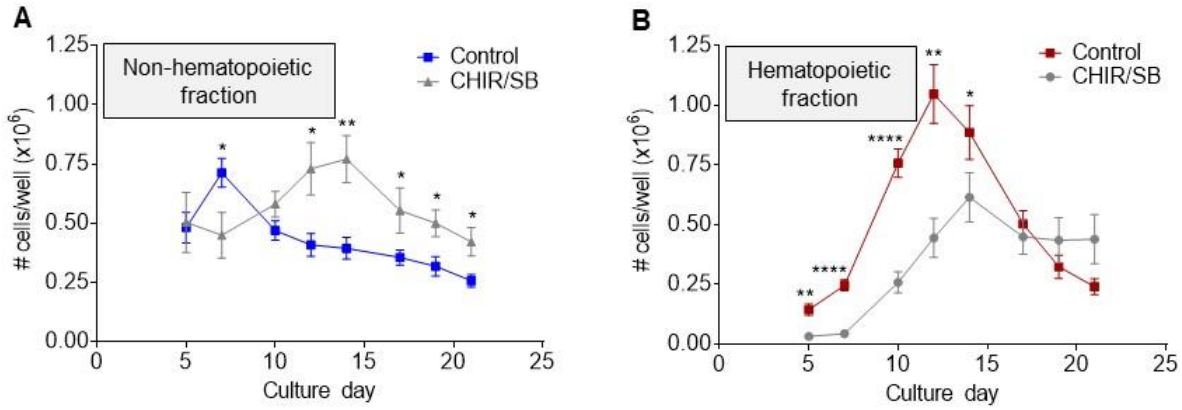

Figure S6 | CHIR/SB molecules increase non-hematopoietic cells and decrease hematopoietic production during human iPSC differentiation with STEMdiff™ hematopoietic kit. (**A**) Absolute numbers of $CD43^{+}CD45^{+/-}$ hematopoietic cells arising from 20-35 iPSC clusters (one well of a 12-well plate) in control and CHIR/SB-supplemented cultures at various days of differentiation (n=6). Associated with Fig. 4A. (**B**) Absolute numbers of $CD43^{-}CD45^{-}$ non-hematopoietic cells arising from 20-35 iPSC clusters (one well of a 12-well plate) in control and CHIR/SB-supplemented cultures at various days of differentiation (n=6). Associated with Fig. 5A. Results are displayed as mean ± SEM. *P<0.05, **P < 0.01, ****P<0.0001, by two-way unpaired Student's t-tests comparing cell numbers in control vs CHIR/SB groups at each culture day.

Table S1 | Human iPSC lines subjected to STEMdiff™ hematopoietic differentiation

Cell line	Type	Starting material	Reprogramming method
MCND-TENS1	Normal control	MPB $CD34^+CD38^-$ cells[(1)]	Sendai virus
MCND-TENS2[(2)]	Normal control	MPB $CD34^+CD38^-$ cells[(1)]	Sendai virus
MCND-TENS3	Normal control	MPB $CD34^+CD38^-$ cells[(1)]	Sendai virus
MCND-S1	Normal control	MPB $CD34^+$ cells[(1)]	Sendai virus
MCND-S3	Normal control	MPB $CD34^+$ cells[(1)]	Sendai virus
NL-5	Normal control	Cord blood $CD34^+$ cells	Episomal plasmid
ND-2	Normal control	Fibroblasts	Episomal plasmid
NC-1	Normal control	Fibroblasts	Episomal plasmid
NC-4	Normal control	Fibroblasts	Episomal plasmid
NC-5	Normal control	Fibroblasts	Episomal plasmid
113-7	Normal control	Fibroblasts	Episomal plasmid
DBA863-S13	DBA[(3)]	Mononuclear blood cells	Sendai virus
DBA869-S1	DBA[(3)]	Mononuclear blood cells	Sendai virus
DBA872-S1	DBA[(3)]	Mononuclear blood cells	Sendai virus

[(1)] Derived from G-CSF mobilized peripheral blood (MPB)
[(2)] Used in this study
[(3)] Diamond Blackfan Anemia (DBA)

Table S2 | Antibodies for flow cytometry analysis and FACS

Antigen	Fluorochrome	Company/Catalogue #	Species	µL/test
CD34	PE-Cy7	BD Pharmingen 560710	Mouse anti-human	10
CD34	PE	BD Pharmingen 555822	Mouse anti-human	20
CD38	APC	BD Pharmingen 555462	Mouse anti-human	20
CD43	BV711	BD OptiBuild™ 743614	Mouse anti-human	5
CD43	FITC	BD Pharmingen 555475	Mouse anti-human	20
CD45	V450	BD Horizon 560367	Mouse anti-human	5
CD45RA	APC-H7	BD Pharmingen 560674	Mouse anti-human	5
CD49f	PE-Cy5	BD Pharmingen 551129	Rat anti-human	20
CD73	PE	BD Pharmingen 550257	Mouse anti-human	20
CD73	FITC	BD Pharmingen 561254	Mouse anti-human	5
CD90	PE-Cy7	BD Pharmingen 561558	Mouse anti-human	5
CD105	AF647	BD Pharmingen 561439	Mouse anti-human	5
CD144	BV605	BD OptiBuild™ 743705	Mouse anti-human	5
CD184	PE-CF594	BD Horizon 562389	Mouse anti-human	5
CD235a	FITC	BioLegend 349104	Mouse anti-human	5
N/A	7-AAD	Thermofisher 00-6993-50	N/A	5

Table S3 | Taqman™ primers and probes

Gene	Assay or sequence	Probe
GAPDH	Life Technologies, Hs03929097_g1	VIC
HoxA5	Life Technologies, Hs00430330_m1	FAM
HoxA9	Life Technologies, Hs00365956_m1	FAM
HoxA10	Life Technologies, Hs00172012_m1	FAM